Chemical Science

ROYAL SOCIETY OF CHEMISTRY

EDGE ARTICLE

View Article Online
View Journal | View Issue



Cite this: *Chem. Sci.*, 2022, **13**, 13147

All publication charges for this article have been paid for by the Royal Society of Chemistry

Received 26th July 2022
Accepted 24th October 2022

DOI: 10.1039/d2sc04168e

rsc.li/chemical-science

# Cyclic arrays of five pyrenes on one rim of a planar chiral pillar[5]arene†

Kenichi Kato, *[a] Shunsuke Ohtani,[a] Masayuki Gon, [b] Kazuo Tanaka [b] and Tomoki Ogoshi *[ac]

Spatial arrangement of multiple planar chromophores is an emerging strategy for molecule-based chiroptical materials *via* easy and systematic synthesis. We attached five pyrene planes to a chiral macrocycle, pillar[5]arene, producing a set of chiroptical molecules in which pyrene-derived absorption and emission were endowed with dissymmetry by effective transfer of chiral information. The chiroptical response was dependent on linker structures and substituted patterns because of variable interactions between pyrene units. One of these hybrids showed larger dissymmetry factor and response wavelength ($g_{lum} = 7.0 \times 10^{-3}$ at *ca.* 547 nm) than reported pillar[5]arene-based molecules using the pillar[5]arene cores as parts of photo-responsive π-conjugated units.

## Introduction

Chirality occurs widely in nature, enabling sophisticated folding or assembling structures and recognition systems that are essential for biological activities. Chirality is also a key for advanced materials because of characteristic functions caused by symmetry breaking. Among them, interaction between chiral compounds and circularly polarized light is of prime importance. Much attention is directed to circular dichroism (CD) and circularly polarized luminescence (CPL) of newly synthesized compounds with diverse structures.[1] Organic π-conjugated molecules are attractive in terms of strong π–π* electronic transitions as well as lightweight, flexible and soluble nature.[2] However, they are mostly achiral due to planar structures and need to be endowed with chirality by structural modification.

Contorting planar π-conjugated skeletons into non-planar ones is a major protocol to attain strong chiroptical response. Helicenes[3] are one of the most representative classes of compounds and have been extensively studied (Fig. 1a), including derivatives with controlled symmetry[4,5] and electric and magnetic transition dipole moments ($\mu$ and $m$).[6] Recently, macrocyclic compounds have also attracted intensive research,[7] one of which improved the record of CPL dissymmetry factors ($g_{lum}$)‡ in organic molecules.[8] Cyclic structures were indicated to be effective for the development of chiroptical molecules because they had appropriate symmetry and an increased ratio of $|m|$ to $|\mu|$, which is typically small in organic compounds without d- and f-electrons. Although these platforms offer appealing electronic systems with smooth π-conjugation, the synthesis requires construction of distorted structures and in some cases fused structures *via* multiple bond formation.

Spatial arrangement of π-conjugated planes is another strategy for chiroptical molecules.[2,9–12] In these systems, π-conjugated units are simply connected to chiral centres with single bonds or aggregate into chiral assembly using non-covalent interactions. These characteristics are suitable for systematic structural alteration, enabling easy tuning of response wavelength and solubility.

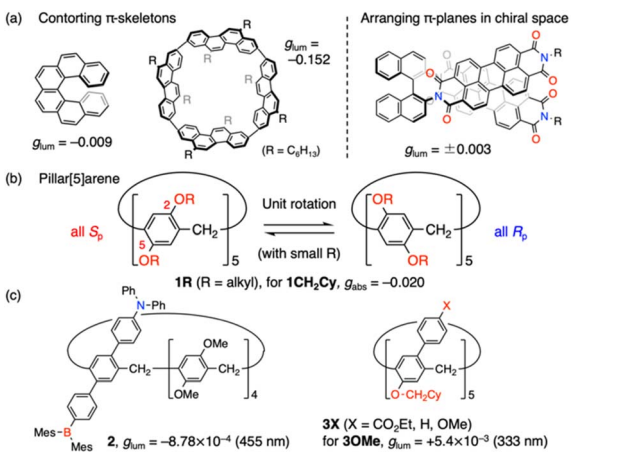


Fig. 1 (a) Two key strategies for chiroptical molecules. (b) Chemical structure of a pillar[5]arene and (c) its modification toward CPL-active derivatives.

[a]*Department of Synthetic Chemistry and Biological Chemistry, Graduate School of Engineering, Kyoto University, Nishikyo-ku, Kyoto, 615-8510, Japan. E-mail: katok@sbchem.kyoto-u.ac.jp; ogoshi@sbchem.kyoto-u.ac.jp*

[b]*Department of Polymer Chemistry, Graduate School of Engineering, Kyoto University, Nishikyo-ku, Kyoto, 615-8510, Japan*

[c]*WPI Nano Life Science Institute, Kanazawa University, Kakuma-machi, Kanazawa, 920-1192, Japan*

† Electronic supplementary information (ESI) available. Experimental procedures, NMR and MS spectral data, HPLC charts and results of optical measurement. See DOI: https://doi.org/10.1039/d2sc04168e

The less rigid structures also allow them to switch the chiroptical properties in response to external stimuli.[9b,d,12] On the other hand, it is relatively difficult to obtain high *g* values with this approach as compared with contorted π-conjugated systems because strong π-conjugation was unavailable for inducing chirality. To transmit chiral information effectively to photo-responsive π-conjugated units, π-stacked dimers in chiral arrangements were extensively used.[9a,c,11] π-Stacked pyrene dimers with excimer emission is one of the most investigated systems[9a] for elaborate stimuli-responsive systems. Meanwhile, molecular designs for strong chiroptical response were rather unexplored. Chiral π-stacked dimers of pyrene were piled up by integrating them with chiral oligo-naphthyl backbones and helical polymers[13] or forming one-dimensional supramolecular assemblies.[14] However, ideas applied in the designs of contorted π-conjugated molecules, such as forming chiral cyclic structures, have not been fully exploited in these π-stacked systems, except the latest example using cyclodextrins.[15] The report attained highly efficient CD and CPL induction, while both left- and right-handed responses were attained by tuning linker units as only one chirality is available for cyclodextrins. Hence, we envisage arranging multiple pyrene units on a rim of pillar[5]arene, a cylindrical macrocyclic molecule.

Pillar[5]arenes **1R** (Fig. 1b)[16,17] are constructed from paraphenylene units linked with methylene groups. Each phenylene unit is usually substituted with alkoxy groups at the 2,5-positions and exhibits planar chirality. With small and flexible alkoxy groups, the π-units can rotate with inversion of the chirality, which affords equilibrium state between energetically preferred all-$S_p$ or all-$R_p$ conformations.[18] On the other hand, two enantiomers are successfully separated when bulky substituents are attached onto both rims.[19] Although enantiopure pillar[5]arenes themselves have good chiroptical properties ($g_{abs}$: $10^{-2}$ order), they are not suitable for CPL materials because of poorly fluorescent nature and short response wavelength (<320 nm). To circumvent these drawbacks, several functionalized pillar[5]arenes were developed (Fig. 1c).[20–22] In 2020, Chen and co-workers introduced amine and borane substituents into one unit of a pillar[5]arene and attained CPL at around 455 nm (**2**).[20a] However, the emission largely relied on the functionalized terphenyl unit and hence limited chiral transfer from the chiral macrocycle core resulted in $10^{-4}$ order of $g_{lum}$ value. We reported a set of rim-differentiated pillar[5]arenes **3X** with improved dissymmetry based on retained $C_5$-symmetry, but the twisted biphenyl units gave chiroptical response at around 400 nm or less.[21] A rational solution to these drawbacks is hybrids with planar π-conjugated units such as pyrene,[23] in which a pillar[5]arene served solely as a chiral $C_5$-symmetric platform. Indeed, a hybrid molecule in the present work exhibited $g_{lum}$ of $-7.1 \times 10^{-3}$ at around 550 nm, derived from a chiral pyrene cluster. The luminescence properties were also dependent on the linker segments and substituents on pyrene rings.

## Results and discussion

### Synthesis and characterization

**Synthesis.** Pillar[5]arene scaffold **9** was prepared according to the reported procedure.[21,24] As an initial attempt, the $S_N2$ reaction with 1-(bromomethyl)pyrene was tested with $Cs_2CO_3$ in a mixture of *N*,*N*-dimethylformamide (DMF) and toluene at 110 °C. Although the target compound was observed in the $^1H$ NMR spectrum, the crude mixture contained large amounts of side products because of the incomplete 5-fold reaction. After several experiments, NaH turned out to be effective but still the target product could not be isolated by gel permeation chromatography (GPC) and repeated recrystallization. The unfunctionalized pyrene segments led to poor solubility in *n*-hexane and low polarity, which made silica gel chromatography useless for purification.

With this partial success in mind, we envisioned incorporation of ester groups on pyrene periphery (Scheme 1). Butyl ester was selected due to its adequate polarity, solubilizing ability and π-stacking character derived from small bulkiness and weakly electron-withdrawing nature. After ester formation with 1-bromobutane,[25] a combination of dichloromethyl methyl ether and $TiCl_4$ enabled to append a formyl group.[26] After reduction of formyl groups into hydroxymethyl groups with $NaBH_4$,[27] three isomers were separated using a high-performance liquid chromatography (HPLC) system with a chiral column. Assignment of isomers **7a–c** was conducted based on their NMR spectra including two-dimensional correlation measurement (for details, see Tables S3-1 and S3-2, Fig. S3-3 to S3-5, S3-12 to S3-16 in the ESI†). Final bromination with $PBr_3$ furnished ester-appended (bromomethyl)pyrenes **8a–c**. The $S_N2$ reaction of pillar[5]arene **9** with **8a–c** was conducted under the conditions optimized with simple (bromomethyl)pyrene. While 1,3-substituted pyrene did not provide the corresponding product at all probably because of large steric hindrance, use of 1,6- and 1,8-derivatives led to smooth reaction due to improved solubility of multi-pyrene products. Since remaining **8b** and **8c** overlapped on silica gel columns, products **10b** and **10c** were obtained as pairs of pure enantiomers in 28–

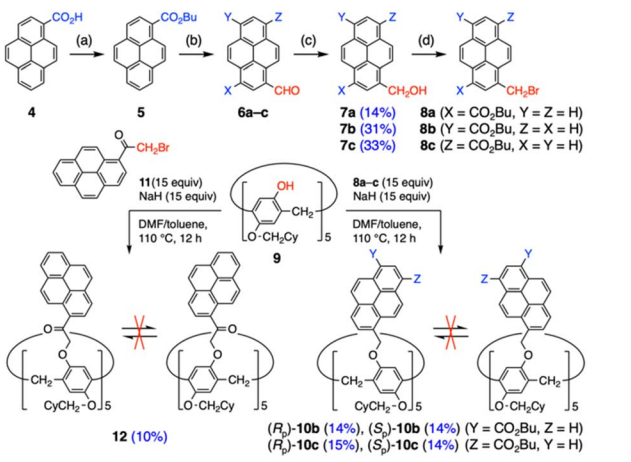


Scheme 1 Introduction of pyrene units on one rim of a pillar[5]arene with cyclohexylmethoxy stoppers. Reagents and conditions: (a) 1-bromobutane (1.5 equiv.), $K_2CO_3$ (2.0 equiv.), DMF, 80 °C, 26 h, quant.; (b) $MeOCHCl_2$ (1.25 equiv.), $TiCl_4$ (1.25 equiv.), $CH_2Cl_2$, 0 °C to RT, 1 h, 46% as mixture; (c) $NaBH_4$ (0.26 equiv.), $CH_2Cl_2$/MeOH, −20 °C, 1 h, total 78%; (d) $PBr_3$ (1.2 equiv.), toluene, 0 °C to RT, 1 h, 44–47%.

29% total yields after chiral HPLC separation (Fig. S6-1†). To examine effects of spacer length between pillar[5]arene and pyrene moieties, **12** was synthesized with 1-(bromoacetyl)pyrene in 10% yield. The solubility of **12** was not very high and hence purification was performed by GPC and recrystallization from $CH_2Cl_2$/*n*-hexane. Because of the inserted carbonyl groups with moderate polarity, **12** was successfully separated into enantiomers using a chiral column.

**NMR spectroscopy.** Because of bulky substituents on both rims of pillar[5]arenes, pyrene-arrayed pillar[5]arenes **10b**, **10c**, and **12** displayed sets of $C_5$-symmetric signals in the $^1$H NMR spectra (Fig. S3-9 to S3-11†). Clear peak splitting was observed for methylene protons in the pillar[5]arene cores and pendent $OCH_2$-moieties on both rims, indicating restricted unit rotation.[18b] Pyrenyl protons appeared at 8.80–6.87 and 9.00–7.55 ppm in **10b** and **10c** respectively, which were largely upfield shifted compared with those in **8b** (9.23–8.03 ppm) and **8c** (9.38–8.00 ppm). The peak shifts were mainly ascribed to aromatic shielding by a pyrene ring in the next unit, suggesting the proximity of pyrene planes suitable for effective interactions.§ Two protons in **12** were much more shielded (6.00 and 5.89 ppm), which implied the existence of CH/π interactions.

## Optical properties

**UV/vis absorption and CD spectra.** Fig. 2a presents the UV/vis absorption and CD spectra of **10b**, **10c** and **12** in $CHCl_3$. Because of five pyrene segments, the UV/vis absorption spectra of **10b** and **10c** were composed of two major bands at 286 and 358 nm with a side peak at 389 nm. In common per-alkoxy-substituted pillar[5]arenes, broad UV absorption was observed at around 300 nm, which was not apparent in **10b** and **10c** by overlapping with the shoulder region of the intense 286 nm peak. In contrast, CD signals due to pillar[5]arene cores were clearly observed at 310 nm with $|\Delta\varepsilon| \sim 120$ M$^{-1}$ cm$^{-1}$ and $|g_{abs}| \sim 4 \times 10^{-3}$ (Table 1). The $|g_{abs}|$ values were smaller than that of the per-cyclohexylmethoxy-substituted derivative ($|g_{abs}| = 20 \times 10^{-3}$)[19] because of dilution by the weakly dissymmetric pyrene-based absorption. From the positive Cotton effect of this peak, the 1st fractions of **10b** and **10c** were assigned as $R_p$-forms and the 2nd fractions as $S_p$-forms. CD intensities in the long-wavelength range were also high for **10b** ($|\Delta\varepsilon| = 83$ M$^{-1}$ cm$^{-1}$ and $|g_{abs}| = 1.0 \times 10^{-3}$ at 372 nm) and moderate for **10c** with some broadening ($|\Delta\varepsilon| = 40$ M$^{-1}$ cm$^{-1}$ and $|g_{abs}| = 0.3 \times 10^{-3}$ at 361 nm). These values indicated that chiral information was transferred effectively from the pillar[5]arene to pyrene moieties in these hybrid molecules.

In **12**, unfunctionalized pyrene rings were separated by longer spacer segments with additional carbonyl groups, but the UV/vis and CD spectra of **12** displayed roughly the same shapes as those of **10b** and **10c**. As minor differences, UV/vis absorption of **12** were broader to extend the tail over 430 nm probably due to the existence of several conformations with different interactions between pyrene units (*vide infra*). Additional CD peaks with the opposite sign were also evident at both high- and low-energy sides of the 310 nm signal. The pyrene-based CD band of **12** was the most intense ($|\Delta\varepsilon| = 97$ M$^{-1}$ cm$^{-1}$ at 373 nm) among the three and reached almost the same dissymmetry as the pillar[5]arene-derived band in the long-wavelength shoulder region ($|g_{abs}| = 2.7 \times 10^{-3}$ at 406 nm).

**Fluorescence and CPL spectra.** Fluorescence spectra of **10b** and **10c** in $CHCl_3$ were composed of single bands with clear vibronic structures at around 400 nm, which can be assigned to emission from locally excited states (Fig. 2b). On the other hand, that of **12** additionally had a weak and broad signal at 500–700 nm. Such bands were almost negligible in the cases of **10b** and **10c**, which reflected the structural differences of spacer lengths. When the excitation wavelength was altered from

Table 1 Summary of chiroptical properties in $CHCl_3$

| | $\lambda_{abs}$ [nm] ($\lvert g_{abs}\rvert \times 10^3$) | | $\Phi_{lum}$[a] | $\lambda_{lum}$[b] [nm] ($\lvert g_{lum}\rvert \times 10^3$) |
|---|---|---|---|---|
| **10b** | 310 (4.0) | 372 (1.0) | 0.13 | (Not detected) |
| **10c** | 310 (3.6) | 361 (0.3) | 0.15 | *ca.* 500 (3.2) |
| **12** | 310 (4.6) | 373 (1.5) | 0.01[c] | *ca.* 547 (7.0)[d] |

[a] $\lambda_{ex} = 350$ nm. [b] $\lambda_{ex} = 280$ nm. [c] $4.4 \times 10^{-6}$ M. [d] $5.7$–$6.5 \times 10^{-6}$ M.

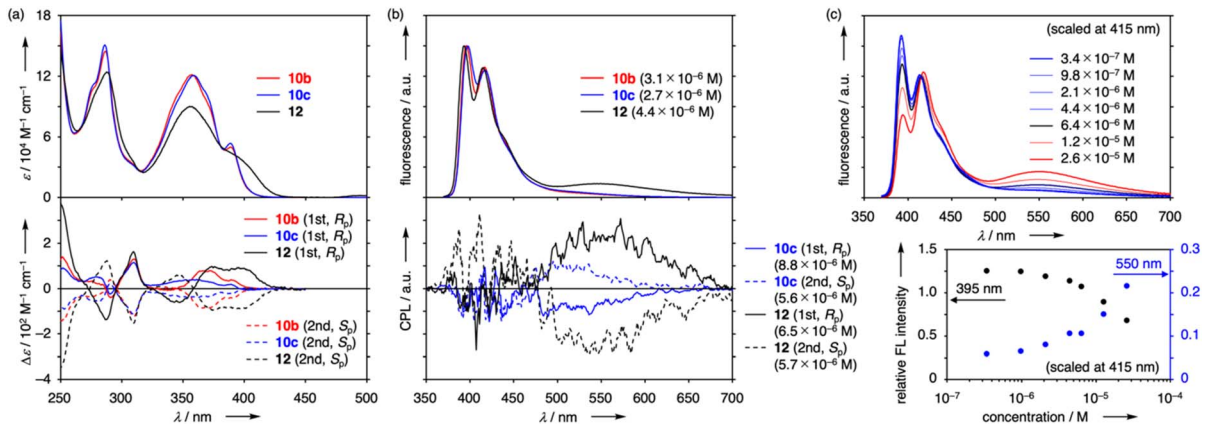


Fig. 2 (a) UV/vis absorption (top) and CD (bottom) spectra of **10b**, **10c** and **12** in $CHCl_3$. (b) Fluorescence (top, $\lambda_{ex} = 350$ nm) and CPL (bottom, $\lambda_{ex} = 280$ nm) spectra of **10b**, **10c** and **12** in $CHCl_3$. (c) Concentration-dependent fluorescence spectra of **12** in $CHCl_3$ (top) and relative intensity plot (bottom) of peaks at 395 nm (black, left axis) and 550 nm (blue, right axis) scaled at 415 nm.

350 nm to 370 and 390 nm, **10b** and **10c** exhibited almost identical spectra to that with 350 nm excitation except for changes in ratios of two peak top intensities (Fig. S5-2†). The spectral shape of **12** varied with small red shifts upon excitation at longer wavelengths, while the intensity at around 547 nm was roughly retained. These results suggested that **10b** and **10c** took nearly single stable conformation, changed between multiple conformations fast or showed similar fluorescence regardless of conformational differences. In contrast, it was assumed that two or more conformers contributed to fluorescence behaviour of **12**, indicating again the significance of spacer structures.

To characterize fluorescent species, excitation spectra were measured for all the peak top wavelengths of **10b**, **10c** and **12** (Fig. S5-3 and S5-4†). While each spectrum of **10b** and **10c** displayed shape like its UV/vis absorption spectrum, that of **12** did not overlap well. Upon detection at 395 and 415 nm, the spectral shape of **12** appeared sharp like those of **10b** and **10c** and it was highly broadened with 550 nm detection. These results implied that the UV/vis absorption spectrum was understood as the sum of two types of excitation spectra and short- and long-wavelength emission were mainly derived from different ground-state conformations. Excitation spectra were also acquired at 500 nm, which corresponded to the tail region of single-pyrene emission. The spectrum of **12** was similar to that at 550 nm, reflecting large contribution of the conformer with broad UV/vis absorption. The spectra of **10b** and **10c** were not as broad as that of **12** but were significantly deviated from excitation spectra at 397 and 417 nm. The broadening indicated the presence of minor conformations in **10b** and **10c** with broad absorption though their populations were too small to be detected in usual UV/vis and fluorescence spectra. Further, two types of species were characterized by emission lifetime measurement (Fig. S5-5 and S5-6, Table S5-1†). At wavelengths of single-pyrene emission, all the hybrids showed lifetimes of 4.3–4.6 ns along with minor contributions with shorter decay constants (0.30–2.3 ns). At 500 nm, **10b** and **10c** had additional components of 22 and 19 ns respectively, which indicated the presence of excimer emission in the tail regions. In the case of **12**, fitting for decay at 500 and 550 nm was rather difficult owing to multiple conformations but included components with longer lifetime (>7.0 ns) assignable to excimer emission. These results demonstrated that conformations with broad absorption led to excimer emission in tail regions more efficiently than those with sharp absorption.

Then, concentration effects on emission properties were investigated. While both UV/vis and fluorescence spectra of **10b** and **10c** were not concentration-dependent, the fluorescence spectrum of **12** changed its shape in response to concentration with its UV/vis, CD, and $^1$H NMR spectral shape unchanged (Fig. S3-18, S5-7 and S6-4†). These results showed the absence of ground-state aggregates. As the concentration increased over $10^{-6}$ M, relative intensity at 395 nm dropped as compared with that of 415 nm and that at 550 nm gradually increased (Fig. 2c). Therefore, long-wavelength emission at around 550 nm was accounted for mainly by intermolecularly formed pyrene excimers. On the other hand, nearly constant intensity (relative intensity of *ca.* 5%) at $3.4 \times 10^{-7}$ M was due to intramolecular excimers. Large contribution of intermolecular excimers implied that most conformations of **12** did not easily take conformations suitable for intramolecular excimer states but were able to form intermolecular π-stacked dimers. On the other hand, absence of concentration-dependence in the fluorescence spectra of **10b** and **10c** indicated that intermolecular excimers were not accessible from **10b** and **10c** probably because of appended ester groups and long-lifetime components in the tail region could be accounted for solely by intramolecular excimers.

CPL spectra were also recorded for enantiopure fractions of **10b**, **10c** and **12** in $CHCl_3$ (Fig. 2b). Notably, single pyrene-based emission at around 400 nm was CPL-silent for all the compounds despite intense CD response and only excimer-based emission showed evident CPL signals. Along this line, **12** displayed a pair of mirror-image CPL at 480–680 nm. The observed $|g_{lum}|$ value at around 547 nm peak top ($7.0 \times 10^{-3}$ at 5.7–6.5 $\times 10^{-6}$ M) was the highest among pillar[*n*]arene single molecules in solution, though the luminescence quantum yield was low ($\Phi_{lum} = 0.01$).¶ The $|g_{lum}|$ value was also concentration-dependent and increased from $2.5 \times 10^{-3}$ at $2.7 \times 10^{-7}$ M to 8.4 $\times 10^{-3}$ at $2.4 \times 10^{-5}$ M, which indicated that CPL signals were composed of both intramolecular and intermolecular excimer emission and the latter possessed larger dissymmetry factor. Curiously, CPL was not detected for **10b** at 350–800 nm but **10c** displayed CPL signals at 470–600 nm ($|g_{lum}| = 3.2 \times 10^{-3}$ at around 500 nm), which corresponded to the tail region with small contribution of intramolecular excimers in the fluorescence spectrum.

## Conclusions

Multiple π-conjugated planes were arranged on a chiral macrocycle by using functionalized pyrenes and a pillar[5]arene with cyclohexylmethoxy groups on the other rim, *via* 5-fold $S_N2$ reactions of a phenolic pillar[5]arene. In these hybrids, fixed chiral information of the pillar[5]arene was effectively transmitted to the assemblies of pyrene units, leading to as intense CD signals at 350–400 nm as that at 310 nm due to the peralkoxy-substituted pillar[5]arene. Pyrene-derived emission bands were composed of single-pyrene fluorescence at around 400 nm with vibronic structures and excimer emission at 500–550 nm in the tail region. The former was silent in CPL response while the latter displayed $10^{-3}$ order of CPL signals. The excimer formation was effective with a three-atom linker as compared with two-atom ones and was sterically hampered when substituents on pyrene units were located inside the macrocycle. Without additional substituents on pyrenes, intramolecular excimer formation competed with the intermolecular process, offering concentration-dependent fluorescence properties.

In this work, a high $|g_{lum}|$ value of $7.0 \times 10^{-3}$ at around 550 nm was attained based on the hybrid of a chiral macrocycle and π-conjugated planes. Although the luminescence quantum yield was low, the obtained CPL response demonstrated a useful design principle for CPL-active pillar[5]arene molecules.

Further studies on chiroptical pillar[*n*]arenes are underway in our group.

## Data availability

The datasets supporting this article have been uploaded as the ESI.†

## Author contributions

K. T. and T. O. supervised and administered this project. K. K. performed conceptualization. K. K., S. O. and M. G. conducted the experiments and theoretical calculations. K. K. prepared the draft and initial version of the ESI,† which were reviewed and edited by all authors.

## Conflicts of interest

There are no conflicts to declare.

## Acknowledgements

This work was supported by JSPS KAKENHI Grant Numbers JP20K22528 (Research Activity Start-up, K. K.), JP21K14611 (Early-Career Scientists, K. K.), JP21K20533 (Research Activity Start-up, S. O.), JP18H04510 and JP20H04670 (Scientific Research on Innovative Areas, T. O.) and JP19H00909 and JP22H00334 (Scientific Research (A), T. O.), JST CREST Grant Number JPMJCR18R3 (T. O.) and the MEXT World Premier International Research Center Initiative (WPI), Japan.

## Notes and references

‡ The dissymmetry factors ($g$) of electronic transitions were described as follows, where $\mu$ and $m$ are electric and magnetic transition dipole moments, respectively, and $\theta$ is the angle between them: $g = \frac{4|\mu||m|cos\ \theta}{|\mu|^2 + |m|^2}$.

§ To gain further structural information, theoretical calculations of the hybrids were performed at the RωB97X-D/6-31G(d,p) and RB3LYP-D3/6-31G(d,p) levels, starting from $C_5$-symmetric geometry without specific inter-unit interactions. However, TD-SCF calculations of the optimized structures failed to give consistent CD spectra for both levels.

¶ To improve luminescence efficiency, optical measurement was also performed in the presence of 1 M adiponitrile.[28] However, UV/vis absorption, CD, fluorescence and luminescence quantum yield measurement did not indicate any differences for **10b**, **10c** and **12**.

1 Reviews on CD, ORD, and CPL: (*a*) J. A. Schellman, *Chem. Rev.*, 1975, **75**, 323; (*b*) F. S. Richardson and J. P. Riehl, *Chem. Rev.*, 1977, **77**, 773; (*c*) J. P. Riehl and F. S. Richardson, *Chem. Rev.*, 1986, **86**, 1.

2 Reviews on organic molecules and their assembly with strong chiroptical response: (*a*) E. M. Sanchez-Carnerero, A. R. Agarrabeitia, F. Moreno, B. L. Maroto, G. Muller, M. J. Ortiz and S. de la Moya, *Chem.–Eur. J.*, 2015, **21**, 13488; (*b*) J. Kumar, T. Nakashima and T. Kawai, *J. Phys. Chem. Lett.*, 2015, **6**, 3445; (*c*) E. Yashima, N. Ousaka, D. Taura, K. Shimomur, T. Ikai and K. Maeda, *Chem. Rev.*, 2016, **116**, 13752.

3 (*a*) R. H. Martin, *Angew. Chem., Int. Ed.*, 1974, **13**, 649; (*b*) Y. Shen and C.-F. Chen, *Chem. Rev.*, 2012, **112**, 1463; (*c*) K. Dhbaibi, L. Favereau and J. Crassous, *Chem. Rev.*, 2019, **119**, 8846.

4 T. Mori, *Chem. Rev.*, 2021, **121**, 2373.

5 (*a*) H. Tanaka, M. Ikenosako, Y. Kato, M. Fujiki, Y. Inoue and T. Mori, *Commun. Chem.*, 2018, **1**, 38; (*b*) H. Tanaka, Y. Kato, M. Fujiki, Y. Inoue and T. Mori, *J. Phys. Chem. A*, 2018, **122**, 7378.

6 Donor–acceptor-type helicenes:(*a*) H. Kubo, T. Hirose and K. Matsuda, *Org. Lett.*, 2017, **19**, 1776; (*b*) H. Kubo, T. Hirose, T. Nakashima, T. Kawai, J.-y. Hasegawa and K. Matsuda, *J. Phys. Chem. Lett.*, 2021, **12**, 686; (*c*) H. Kubo, T. Hirose, D. Shimizu and K. Matsuda, *Chem. Lett.*, 2021, **50**, 804.

7 M. Hasegawa, Y. Nojima and Y. Mazaki, *ChemPhotoChem*, 2021, **5**, 1042.

8 S. Sato, A. Yoshii, S. Takahashi, S. Furumi, M. Takeuchi and H. Isobe, *Proc. Natl. Acad. Sci. U. S. A.*, 2017, **114**, 13097.

9 (*a*) Y. Ohishi and M. Inouye, *Tetrahedron Lett.*, 2019, **60**, 151232; (*b*) J.-L. Ma, Q. Peng and C.-H. Zhao, *Chem.–Eur. J.*, 2019, **25**, 15441; (*c*) Y. Imai, *Chem. Lett.*, 2021, **50**, 1131; (*d*) J. Zhao and P. Xing, *ChemPhotoChem*, 2021, **6**, e202100124.

10 (*a*) N. Harada and K. Nakanishi, *J. Am. Chem. Soc.*, 1969, **91**, 3989; (*b*) N. Harada, Y. Takuma and H. Uda, *J. Am. Chem. Soc.*, 1976, **98**, 5408.

11 (*a*) T. Kawai, K. Kawamura, H. Tsumatori, M. Ishikawa, M. Naito, M. Fujiki and T. Nakashima, *ChemPhysChem*, 2007, **8**, 1465; (*b*) K. Nakabayashi, T. Amako, N. Tajima, M. Fujiki and Y. Imai, *Chem. Commun.*, 2014, **50**, 13228; (*c*) H. Ito, H. Sakai, Y. Okayasu, J. Yuasa, T. Mori and T. Hasobe, *Chem.–Eur. J.*, 2018, **24**, 16889.

12 (*a*) P. Reiné, J. Justicia, S. P. Morcillo, S. Abbate, B. Vaz, M. Ribagorda, Á. Orte, L. Álvarez de Cienfuegos, G. Longhi, A. G. Campaña, D. Miguel and J. M. Cuerva, *J. Org. Chem.*, 2018, **83**, 4455; (*b*) Y. Hashimoto, T. Nakashima, J. Kuno, M. Yamada and T. Kawai, *ChemNanoMat*, 2018, **4**, 815; (*c*) A. Homberg, E. Brun, F. Zinna, S. Pascal, M. Gorecki, L. Monnier, C. Besnard, G. Pescitelli, L. D. Bari and J. Lacour, *Chem. Sci.*, 2018, **9**, 7043; (*d*) K. Takaishi, K. Iwachido and T. Ema, *J. Am. Chem. Soc.*, 2020, **142**, 1774; (*e*) S. Ito, R. Sekine, M. Munakata, M. Asami, T. Tachikawa, D. Kaji, K. Mishima and Y. Imai, *ChemPhotoChem*, 2021, **5**, 920; (*f*) H. Nian, L. Cheng, L. Wang, H. Zhang, P. Wang, Y. Li and L. Cao, *Angew. Chem., Int. Ed.*, 2011, **60**, 15354.

13 (*a*) K. Takaishi, R. Takehana and T. Ema, *Chem. Commun.*, 2018, **54**, 1449; (*b*) K. Takaishi, K. Iwachido, R. Takehana, M. Uchiyama and T. Ema, *J. Am. Chem. Soc.*, 2019, **141**, 6185; (*c*) K. Takaishi, S. Murakami, K. Iwachido and T. Ema, *Chem. Sci.*, 2021, **12**, 14570; (*d*) Y. Nagata, T. Nishikawa and M. Suginome, *Chem. Commun.*, 2012, **48**, 11193.

14 (*a*) J. Xiao, J. Xu, S. Cui, H. Liu, S. Wang and Y. Li, *Org. Lett.*, 2008, **10**, 645; (*b*) A. L. Nussbaumer, D. Studer, V. L. Malinovskii and R. Häner, *Angew. Chem., Int. Ed.*, 2011, **50**, 5490; (*c*) M.-C. Li, H.-F. Wang, C.-H. Chiang,

Y.-D. Lee and R.-M. Ho, *Angew. Chem., Int. Ed.*, 2014, **53**, 4450; (*d*) Z. Wang, A. Hao and P. Xing, *Angew. Chem., Int. Ed.*, 2020, **59**, 11556.

15 H. Shigemitsu, K. Kawakami, Y. Nagata, R. Kajiwara, S. Yamada, T. Mori and T. Kida, *Angew. Chem., Int. Ed.*, 2022, **61**, e202114700.

16 T. Ogoshi, S. Kanai, S. Fujinami, T.-a. Yamagishi and Y. Nakamoto, *J. Am. Chem. Soc.*, 2008, **130**, 5022.

17 Reviews and a book on pillar[*n*]arenes:(*a*) P. J. Cragg and K. Sharma, *Chem. Soc. Rev.*, 2012, **41**, 597; (*b*) M. Xue, Y. Yang, X. Chi, Z. Zhang and F. Huang, *Acc. Chem. Res.*, 2012, **45**, 1294; (*c*) N. L. Stutt, H. Huacheng, S. T. Schneebeli and J. F. Stoddart, *Acc. Chem. Res.*, 2014, **47**, 2631; (*d*) K. Yang, Y. Pei, J. Wen and Z. Pei, *Chem. Commun.*, 2016, **52**, 9316; (*e*) T. Ogoshi, T.-a. Yamagishi and Y. Nakamoto, *Chem. Rev.*, 2016, **116**, 7937; (*f*) S. Fa, T. Kakuta, T.-a. Yamagishi and T. Ogoshi, *Chem. Lett.*, 2019, **48**, 1278; (*g*) J.-F. Chen, J.-D. Ding and T.-B. Wei, *Chem. Commun.*, 2021, **57**, 9029; (*h*) *Pillararene*, ed. T. Ogoshi, The Royal Society of Chemistry, Cambridge, U.K., 2016.

18 (*a*) T. Ogoshi, K. Kitajima, T. Aoki, S. Fujinami, T.-a. Yamagishi and Y. Nakamoto, *J. Org. Chem.*, 2010, **75**, 3268; (*b*) K. Du, P. Demay-Drouhard, K. Samanta, S. Li, T. U. Thikekar, H. Wang, M. Guo, B. v. Lagen, H. Zuilhof and A. C.-H. Sue, *J. Org. Chem.*, 2020, **85**, 11368.

19 T. Ogoshi, K. Masaki, R. Shiga, K. Kitajima and T.-a. Yamagishi, *Org. Lett.*, 2011, **13**, 1264.

20 (*a*) J.-F. Chen, X. Yin, B. Wang, K. Zhang, G. Meng, S. Zhang, Y. Shi, N. Wang, S. Wang and P. Chen, *Angew. Chem., Int. Ed.*, 2020, **59**, 11267; (*b*) H. Zhu, Q. Li, B. Shi, H. Xing, Y. Sun, S. Lu, L. Shangguan, X. Li, F. Huang and P. J. Stang, *J. Am. Chem. Soc.*, 2020, **142**, 17340; (*c*) J.-F. Chen, X. Yin, K. Zhang, Z. Zhao, S. Zhang, N. Zhang, N. Wang and P. Chen, *J. Org. Chem.*, 2021, **86**, 12654.

21 K. Kato, Y. Kurakake, S. Ohtani, S. Fa, M. Gon, K. Tanaka and T. Ogoshi, *Angew. Chem., Int. Ed.*, 2022, **61**, e202209222.

22 Chiroptical supramolecular systems using pillar[*n*]arenes:(*a*) W.-J. Li, Q. Gu, X.-Q. Wang, D.-Y. Zhang, Y.-T. Wang, X. He, W. Wang and H.-B. Yang, *Angew. Chem., Int. Ed.*, 2021, **60**, 9507; (*b*) S. Fa, T. Tomita, K. Wada, K. Yasuhara, S. Ohtani, K. Kato, M. Gon, K. Tanaka, T. Kakuta, T.-a. Yamagishi and T. Ogoshi, *Chem. Sci.*, 2022, **13**, 5846.

23 Pyrene units were incorporated into pillar[*n*]arene racemates:(*a*) N. L. Strutt, R. S. Forgan, J. M. Spruell, Y. Y. Botros and J. F. Stoddart, *J. Am. Chem. Soc.*, 2011, **133**, 5668; (*b*) T. Ogoshi, R. Shiga, M. Hashizume and T.-a. Yamagishi, *Chem. Commun.*, 2011, **47**, 6927; (*c*) T. Ogoshi, D. Yamafuji, D. Kotera, T. Aoki, S. Fujinami and T.-a. Yamagishi, *J. Org. Chem.*, 2012, **77**, 11146; (*d*) T. Ogoshi, D. Yamafuji, T.-a. Yamagishi and A. M. Brouwer, *Chem. Commun.*, 2013, **49**, 5468; (*e*) C. Penga, W. Liangb, J. Jia, C. Fana, K. Kanagaraja, W. Wua, G. Chenga, D. Sua, Z. Zhonga and C. Yang, *Chin. Chem. Lett.*, 2021, **32**, 345.

24 (*a*) J. Ding, J. Chen, W. Mao, J. Huang and D. Ma, *Org. Biomol. Chem.*, 2017, **15**, 7894; (*b*) M. Guo, X. Wang, C. Zhan, P. Demay-Drouhard, W. Li, K. Du, M. A. Olson, H. Zuilhof and A. C.-H. Sue, *J. Am. Chem. Soc.*, 2018, **140**, 74; (*c*) P. Demay-Drouhard, K. Du, K. Samanta, X. Wan, W. Yang, R. Srinivasan, A. C.-H. Sue and H. Zuilhof, *Org. Lett.*, 2019, **21**, 3976; (*d*) K. Du and A. C.-H. Sue, *Synlett*, 2019, **30**, 2209.

25 Q. Kong, W. Zhuang, G. Li, Y. Xu, Q. Jiang and Y. Wang, *New J. Chem.*, 2017, **41**, 13784.

26 (*a*) T. Yamato, A. Miyazawa and M. Tashiro, *J. Chem. Soc., Perkin Trans. 1*, 1993, 3127; (*b*) K. S. Unikela, B. L. Merner, P. G. Ghasemabadi, C. C. Warford, C. S. Qiu, L. N. Dawe, Y. Zhao and G. J. Bodwell, *Eur. J. Org. Chem.*, 2019, 4546.

27 P. Skrinjar, M. Schwarz, S. Lexmüller, T. P. Mechtler, M. Zeyda, S. Greber-Platzer, J. Trometer, D. C. Kasper and H. Mikula, *ACS Cent. Sci.*, 2018, **4**, 1688.

28 X. Shu, S. Chen, J. Li, Z. Chen, L. Weng, X. Jia and C. Li, *Chem. Commun.*, 2012, **48**, 2967.